PERGAMON

Solid State Communications 123 (2002) 33–36

solid state communications

www.elsevier.com/locate/ssc

Carbon nano-ribbons and their edge phonons

T. Tanaka[a,b,*], A. Tajima[a,b], R. Moriizumi[a,b], M. Hosoda[a,b], R. Ohno[a,b], E. Rokuta[a,b,1], C. Oshima[a,b], S. Otani[c]

[a]*Department of Applied Physics, Waseda University, 3-4-1 Okubo, Shinjuku, Tokyo 169-8555, Japan*
[b]*Kagami Memorial Laboratory for Materials Science and Technology, Waseda University, 2-8-26, Nishi-Waseda, Shinjuku, Tokyo 169-0051, Japan*
[c]*National Institute for Researches in Inorganic Materials, 1-1 Namiki, Tsukuba, Ibaraki 305-0044, Japan*

Received 8 January 2002; accepted 30 April 2002 by S. Ushioda

Abstract

Well-defined carbon nano-ribbons with a honeycomb structure have been grown on a TiC (755) surface. The width between two armchair edges is ~1.3 nm and the length is a macroscopic scale. The phonon modes and the electronic π bands of the carbon nano-ribbons were quantized, which is a characteristic feature of the ribbons with nano-scale widths. Additionally, we have detected the transverse optical edge phonons, of which the vibrational amplitudes are localized at the armchair edge sites. © 2002 Elsevier Science Ltd. All rights reserved.

PACS: 81.07.Bc; 63.22. + m; 68.35.Ja; 82.80.Pv

Keywords: A. Nanostructures; Epitaxy; Phonons; Electron energy loss spectroscopy

Modern nano-carbon systems such as fullerenes and carbon nano-tubes have received tremendously large attention in the research fields of material science. The theoretical and experimental works have clarified their interesting properties. In the practical applications, on the other hand, classical nano-carbon systems including charcoal, activated carbon fibers and the other non-crystalline carbons have been widely used as absorbers of poison molecules in polluted air and water, and they are recently applied to the anodes in the high-capacity Li-ion batteries for a cellular telephone, notebook-type PC, and hybrid vehicle. The difference between the modern and classical nano-carbon systems is large areas of edge sites, which produces the affinity of gas adsorption and Li chemisorption.

Recently, carbon nano-ribbons as shown in Fig. 1 were discussed as a theoretical model for understanding the classical nano-carbon systems because of both the simple edge shape and the large area of edge sites [1–3]. The theorists predicted the edge-localized states related to the affinity of adsorption; the localized edge states of phonons exist at armchair edges, not at the zigzag edges [1]. On the contrary, electronic edge states of π electrons exist at zigzag edges, not at the armchair edges [2].

From experimental point of view, however, the basic properties of the classical nano-carbon systems are not clearly understood because no well-defined specimens existed so far; even atomic structures of the systems are not clarified. In this work, we have reported well-defined carbon nano-ribbons with the width of ~1.3 nm and the armchair edges as shown in Fig. 1. The nano-ribbons possess the large area of edge sites as the common feature of the classical nano-carbon systems. In addition, we detected the localized edge phonons, which were predicted theoretically in nano-ribbons with the armchair edges [1].

A chemical vapor deposition (CVD) method is widely used for growth of uniform and epitaxial graphene sheets [4]. The graphene sheets on various solid surfaces are formed by dehydrogenation of hydrocarbons such as ethylene, benzene, etc. Nano-ribbon-like structures were

* Corresponding author. Address: Kagami Memorial Laboratory for Materials Science and Technology, Waseda University, 2-8-26, Nishi-Waseda, Shinjuku, Tokyo 169-0051, Japan. Tel.: +81-3-5286-3784; fax: +81-3-3205-1353.
E-mail address: 60115085@mn.waseda.ac.jp (T. Tanaka).
[1] Present address: Institutes of Scientific and Industrial Research, Osaka University, Mihogaoka 8-1, Ibaraki, Osaka 567-0047, Japan.

0038-1098/02/$ - see front matter © 2002 Elsevier Science Ltd. All rights reserved.
PII: S0038-1098(02)00186-2

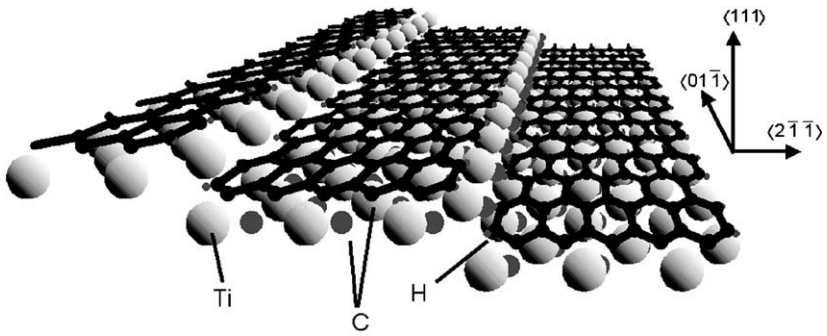

Fig. 1. Schematic of the carbon nano-ribbons on TiC (755).

sometimes observed in STM images [5,6]. Fig. 2 shows one example; carbon nano-ribbons with a 1 nm width grew at the step edge of the large terrace, and the sheets are cut compulsorily at the edge. If we adjust the terrace width, hence, we expect to control the ribbon widths. Recently, we tried to grow the nano-ribbons on various step surfaces, and on TiC (755) we have grown successfully the well-defined nano-ribbons with a uniform width. Unfortunately, we did not succeed to observe a STM image of nano-ribbons because of our technical problems, but the atomic structure of nano-ribbons was confirmed by LEED, and the phonon spectra were measured by high resolution electron energy loss spectroscopy (HREELS).

Clean TiC (755) surfaces were prepared in the conventional way as follows. The specimens were cut from a large single-crystal rod with a spark-erosion-cutting tool combined with a Laue X-ray camera. The accuracy of the crystal orientation was below $\pm 1°$. The surface was polished mechanically to optical finish, and the clean surface was obtained by heating up to 1700 K in UHV. The LEED patterns indicated that the clean surface possesses regular (111) terraces of $\sim$1.3 nm in width and

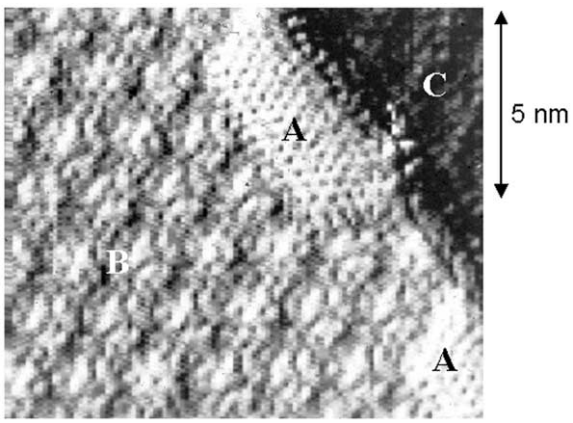

Fig. 2. An STM image of carbon nano-ribbons grown in region (A) along a step edge between the graphene-covered terrace (B) and the same lower terrace (C) [5]. The moiré pattern observed on both the terraces is due to the overlapping of two periodicities of a monolayer graphene overlayer and TaC (111) substrate.

macroscopic lengths as shown in Fig. 1. Similarly to the clean TiC (111) surface [7], the topmost atoms on the terraces of TiC (755) were Ti.

For the growth of graphene sheets, the clean surface above 1100 K was exposed to benzene (C_6H_6) molecules for $\sim$200 l. An additional C 1s peak appeared in the XPS spectra; the peak intensity indicated monolayer thickness of the carbon layer, and the binding energy of 285 eV exhibits formation of graphitic C–C bonds. Fig. 3 shows a typical LEED pattern of the graphene-covered surface. The pattern consists of diffraction spots from the terraces and the graphene sheets with nano-scale widths. The LEED pattern indicates clearly the growth of a graphene sheet with the following epitaxial relation; graphene ⟨0001⟩//TiC ⟨111⟩ and graphene ⟨1200⟩//TiC⟨011⟩. That is to say, the direction of the step edge line is parallel to the armchair edge direction of the graphene sheet as shown in Fig. 1. The ribbon width is about five times as large as the size of a C hexagon ring. The diffraction spots of the graphene are not circular but ellipsoidal, which shows clearly the anisotropic arrangement of carbon atoms in the nano-ribbons. Though the similar ellipsoidal diffraction spots from substrate were observed in Fig. 3, the origin of the ellipsoidal spots is different. Some ellipsoidal spots are formed by overlapping of two nearest-neighbor spots due to the interference of the beams reflected from the different terrace as shown in Fig. 2.

The additional evidence for nano-ribbon growth was observed in both the vibrational and electronic spectra. Since one-dimensional periodicity of the nano-ribbons guarantees the conservation law of the wavevector k parallel to the periodic direction, we measured the k-resolved phonon spectrum by HREELS and the k-resolved electronic spectra by angle-resolved ultraviolet photoemission spectroscopy (ARUPS).

Fig. 4 shows typical k-resolved phonon spectra of both the carbon nano-ribbon at $k = 0.72$ Å^{-1} and a macroscopic graphene sheet at $k = 0.75$ Å^{-1} by means of HREELS. In contrast to the isolated intense peaks in the spectra of the macroscopic sheet, only broad bands are observed on the nano-ribbons. This is a clear experimental indication of nano-ribbon formation, because of the energy resolution not high enough to resolve the many quantized phonon

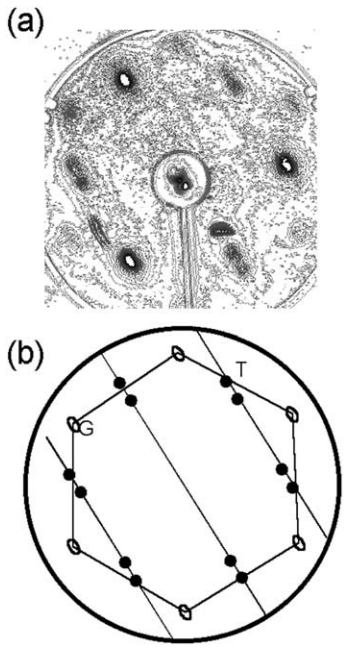

Fig. 3. (a) LEED pattern of carbon nano-ribbon on TiC (755). $E_0 = 75$ eV. (b) The schematic view of picture (a). The diffraction spots 'G' depicted by open circles come from carbon nano-ribbon, and all the other ones 'T' depicted by solid circles are the spots of the substrate.

branches, which result from the nano-scale width of the nano-ribbons. The two bands of the phonons with perpendicular displacement around 40 and 75 meV indicate the softened graphene lattice, which is observed in monolayer graphene on different substrate [8]. The Rayleigh

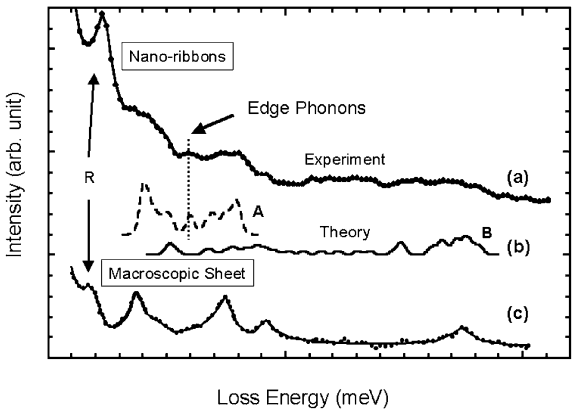

Fig. 4. (a) Typical vibrational spectrum of the nano-ribbons at $k = 0.72$ Å^{-1}. (b) The calculated spectra. The curve A depicted by a broken curve is the vibrational modes with perpendicular polarizations, and curve B depicted by a solid curve is the one with the horizontal polarizations. The dotted line indicates the energy position of the edge phonon. (c) Typical vibrational spectrum of a macroscopic graphene sheet at $k = 0.75$ Å^{-1}. Rayleigh modes are indicated by R.

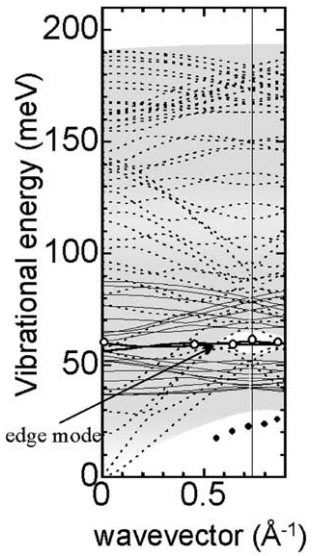

Fig. 5. Experimental and theoretical phonon dispersion relation of the carbon nano-ribbons. The open circles represent the observed edge modes, and the gray area represents the detected phonon bands. The filled circles indicate the observed Rayleigh waves related to the substrate [9]. The calculated results are shown for the phonon modes with the perpendicular polarization (broken curve) except the edge mode (solid curve) and the horizontal polarization (dotted curve). The force constant model for the calculation is explained in the text.

mode at ~20 meV denoted by R in Fig. 4 is acoustic phonon mainly localized in the outermost layer of TiC substrate [8].

For comparison, the theoretical density of states (DOS) of nano-ribbons at $k = 0.72$ Å^{-1} is depicted as the spectrum (b) in Fig. 4. The broken curve (A) is the vibrational modes with perpendicular polarizations to the layer, and the solid curve (B) is the vibrational ones with horizontal polarizations. The phonons of nano-ribbons of ~1.3 nm in width with armchair edges were calculated by using a force constant model. Since the previous calculation [1] did not contain softening of a graphene lattice, which occurred in this system, we calculated them on the basis of a model proposed by Aizawa et al. [8]. The spectrum (b) was finally obtained by the convolution of the calculated DOS and a Gaussian function with a 4 meV width expressing the energy resolution. The spectrum (b) explains well the observed continuous spectrum, which supports strongly the quantization of the phonons.

Furthermore, we found a tiny phonon peak, of which the vibrational energy agrees with the calculated one of the edge states depicted by the dotted line in Fig. 4. The observed energy is also consistent with the other experimental data concerning the edge phonons of an *h*-BN sheet [9].

Fig. 5 shows the phonon dispersion relation of the nano-ribbons obtained from angle resolved HREEL spectra. The observed bands depicted by gray area agree with the calculated quantized branches depicted by dotted and

broken curves. In addition, some data points plotted by open circles agree well with the branches of the edge states shown by solid curves. According to the theoretical calculation, appearance of edge states supports the edge of the nano-ribbons with armchair edges. The theory was also confirmed in the electronic states. The quantized electronic π states and no edge π states were observed in ARUPS measurements [10].

In summary, all the observed data of LEED, AES, XPS, ARUPS and HREELS are consistent with the growth of the carbon nano-ribbons with $\sim$1.3 nm widths. The quantization of the phonons and electronic π states supports the nano-scale width. The detection of the edge phonon and no appearance of edge π state indicate armchair edges of the ribbons on TiC (755), which are consistent with LEED results.

Acknowledgments

This work was supported by special coordination funds for Promoting Science and technology, by the Ministry of ESSC and by Research for the Future in JSPS.

References

[1] M. Igami, M. Fujita, S. Mizuno, Appl. Surf. Sci. 130–132 (1998) 870.
[2] M. Fujita, K. Wakabayashi, K. Nakada, J. Phys. Soc. Jpn 65 (1996) 1920.
[3] K. Wakabayashi, M. Fujita, H. Ajiki, M. Sigrist, Phys. Rev. B 59 (1999) 8271.
[4] C. Oshima, A. Nagashima, J. Phys.: Condens. Matter 9 (1997) 1.
[5] A. Nagashima, H. Itoh, T. Ichinokawa, S. Otani, C. Oshima, Phys. Rev. B 50 (1994) 4756.
[6] R. Koch, O. Haase, M. Borbonus, K.H. Rieder, Phys. Rev. B 45 (1992) 1525.
[7] C. Oshima, M. Aono, S. Otani, Y. Ishizawa, Solid State Commun. 48 (1983) 911.
[8] T. Aizawa, R. Souda, S. Otani, Y. Ishizawa, C. Oshima, Phys. Rev. B 42 (1990) 11469.
[9] T. Tanaka, C. Oshima, in press.
[10] R. Ohno, M. Hosoda, T. Tanaka, S. Otani, C. Oshima, in press.